Inverse Problems, Design and Optimization Symposium
Rio de Janeiro, Brazil, 2004

THE VARIATION OF THE METAL/MOLD HEAT TRANSFER COEFFICIENT ALONG THE CROSS SECTION OF CYLINDRICAL SHAPED CASTINGS

Eduardo N. Souza, Noé Cheung, Carlos A. Santos, Amauri Garcia
Department of Materials Engineering
State University of Campinas, UNICAMP
Campinas, SP, Brazil
edusouza@fem.unicamp.br
cheung@fem.unicamp.br
alex@fem.unicamp.br
amaurig@fem.unicamp.br

ABSTRACT

During solidification, the mathematical analysis of heat flow depends on the transient heat transfer coefficient at the metal/mold interface. The analysis of heat transfer behavior along a cylindrical section is necessary for a better control of solidification in conventional foundry and continuous casting processes. For this purpose, a water-cooled experimental apparatus was developed, and experiments were carried out with SnPb alloys with different melt superheats. The heat transfer coefficients were determined by a theoretical-experimental fit of thermal profiles (IHCP). The results have shown a variation in heat flow conditions along the metal/mold interface provoked by the action of solidification thermal contraction connected with the gravitational effect. In macrostructural terms, this effect was evident with an asymmetric structure due to the variation of metal/mold thermal contact along the cylinder cross section. Experimental equations correlating heat transfer coefficients as a power function of time along the cross section of cylindrical horizontal castings of Sn-Pb alloys are proposed.

NOMENCLATURE

c: specific heat	[J/kg.K]
h : interface heat transfer coefficient	[W/m^{2}K]
k : thermal conductivity	[W/m.K]
K_o: partition coefficient	
L: latent heat of fusion	[J/kg]
$\dot{q}$: internal heat generation	[J/Kg]
T : temperature	[ºC]
ΔT: melt superheat	[ºC]
T_E: eutetic temperature	[ºC]
T_F: fusion temperature	[ºC]
T_L: liquidus temperature	[ºC]
T_P: pouring temperature	[ºC]
Ta: ambient temperature	[ºC]
t : time	[s]
e: mold wall tickness	[m]

Greek symbols

ρ : density	[kg/m^3]

Subscripts

L : liquid
S : solid
W : water
m : mold
M/m : metal/mold

INTRODUCTION

The metal's contraction phenomenon, the physical and chemical characteristics of both metal and mold, and the mold expansion during solidification, are mechanisms, which are responsible for the air gap formation in the metal/mold interface. In the beginning of the process, when the metal is completely liquid, the thermal contact is more effective due to the higher fluidity and the metalostatic pressure effects. However, with the evolution of solidification, the thermal contraction generated by the liquid/solid transformation creates a physical space at the interface, increasing in this way, the thermal resistance to the heat flowing into the mold. Some experimental studies [1,2,3] have determined the transient heat transfer coefficient at the metal/mold interface (hi) in cylindrical ingots, but they have not considered the angular variation of the gap along the cross section.

In the horizontal continuous casting, the air gap at the metal/mold interface varies from the bottom to the top of the transverse section[4], with a more effective contact at the bottom, decreasing as it moves toward the top (figure 1). As a consequence, an asymmetric granular macrostructure will be produced. The analysis of the interfacial heat transfer behavior along the cross section of a cylindrical ingot has as main objective to improve the solidification control by means of mathematical models.

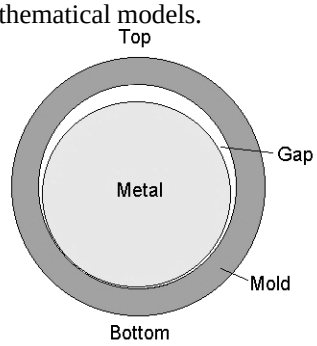

Figure 1. Interfacial gap variation along a cylindrical cross section.

MATHEMATICAL ANALYSIS

The development of the mathematical model is based on the general equation of heat conduction[5] expressed in cylindrical coordinates:

$$\frac{1}{r}.\frac{\partial}{\partial r}\left(kr.\frac{\partial T}{\partial r}\right)+\frac{1}{r^2}.\frac{\partial}{\partial \phi}\left(k.\frac{\partial T}{\partial \phi}\right)+\frac{\partial}{\partial z}\left(k.\frac{\partial T}{\partial z}\right)+\dot{q}=\rho c.\frac{\partial T}{\partial t} \quad (1)$$

r, z and ϕ are the cylindrical coordinates represented in figure 2. The term of the heat generation of energy (q) in the unsteady state condition is:

$$\dot{q} = r.L.\frac{\partial fs}{\partial t} \quad (2)$$

where:

- ∂fs , it is the fraction of solid formed during the phase transformation;

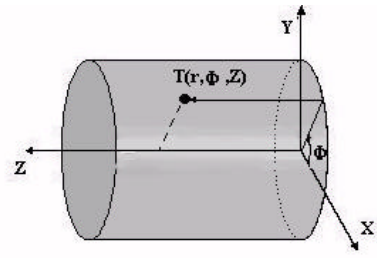

Figure 2. Cylindrical coordinate system.

Considering that the flow of heat is mostly radial, equation (1) can be reduced for the one-dimensional form. Thus, the direction z of heat extraction can be neglected, once it is not significant regarding the heat flow in the r and ϕ directions. In the case of ingots with a symmetrical section, the heat flow in the ϕ direction can also be neglected, resulting in a simplified equation.

$$\frac{1}{r}.\frac{\partial}{\partial r}\left(k.r.\frac{\partial T}{\partial r}\right)+ r.L.\frac{\partial fs}{\partial t} = r.c.\frac{\partial T}{\partial t} \quad (3)$$

Expanding the partial derivatives in relation to the radius and considering the material as isotropic (a constant k in equation 3), it follows that:

$$k.\left(\frac{\partial^2 T}{\partial r^2}+\frac{1}{r}.\frac{\partial T}{\partial r}\right)+ r.L.\frac{\partial fs}{\partial t} = r.c.\frac{\partial T}{\partial t} \quad (4)$$

Rearranging equation (4), it follows:

$$k.\left(\frac{\partial^2 T}{\partial r^2}+\frac{1}{r}.\frac{\partial T}{\partial r}\right)= r.\frac{\partial T}{\partial t}.\left(c - L.\frac{\partial fs}{\partial T}\right) \quad (5)$$

where:

$$c' = \left(c - L.\frac{\partial fs}{\partial T}\right) \quad (6)$$

By defining a term c', known as the pseudo specific heat, which is responsible for the latent heat liberation effect during the phase transformation, the cylindrical coordinates equation is reduced to:

$$\frac{k}{r.c'}.\left(\frac{\partial^2 T}{\partial r^2}+\frac{1}{r}.\frac{\partial T}{\partial r}\right)=.\frac{\partial T}{\partial t} \quad (7)$$

The terms k, ρ, c ' vary in agreement with the phase in that the metal meet.

Using the finite difference method (FDM) for the development of equation (7), we have:

$$T_i^{n+1}=\frac{k_i.\Delta t}{r_i.c_i'}\left[\frac{T_{i-1}^n-2T_i^n+T_{i+1}^n}{\Delta r^2}+\frac{1}{r_i}.\left(\frac{T_{i+1}^n-T_{i-1}^n}{2\Delta r}\right)\right]+T_i^n \quad (8)$$

for $i \neq 0$.

Or:

$$T_i^{n+1} = \frac{\Delta t}{r_i . c_i . r_i . \Delta r^2} . \left[k . r_{i-\frac{1}{2}} . \left(T_{i-1}^n - T_i^n \right) + k . r_{i+1} . \left(T_{i+\frac{1}{2}}^n - T_i^n \right) \right] + T_i^n \quad (9)$$

Where the subscript (i) represents the location of the element in the finite difference mesh and (n+1), the instant in that the nodal temperature is being calculated, as represented in the nodal network shown in figure 3.

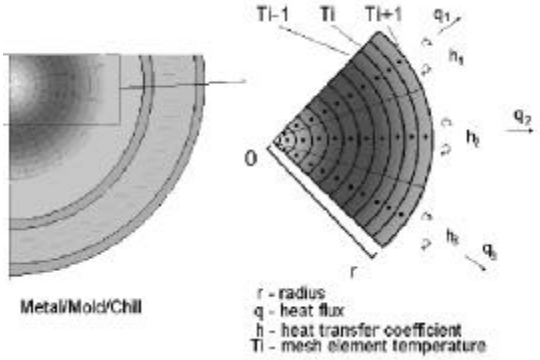

Figure 3. FDM mesh applied at the cross section of the metal/mold cylindrical system.

Considering the metal/mold interface, the following thermal balance can be applied:

$$T_{M/m}^{n+1} = \frac{\Delta t}{r . c . r_m . \Delta r} \left[h r . \left(T_a^n - T_m^n \right) + k . r_{m-\frac{1}{2}} . \frac{T_{m-1}^n - T_m^n}{\Delta r} \right] + T_{M/m}^n \quad (10)$$

where:

- r_m , it is external radius of the cylindrical ingot;
- $T_{M/m,}$ is the metal/mold interface temperature;
- h, it is the overall heat transfer coefficient between the casting surface and the coolant fluid:

$$\frac{1}{h} = \frac{1}{h_{M/m}} + \frac{e}{k_m} + \frac{1}{h_W} \quad (11)$$

As the solidification proceeds, the contraction of the metal increases forming an air gap at the metal/mold interface, increasing the thermal resistance with the consequent decrease in heat flow. The knowledge of the transient heat transfer coefficient at the metal/mold interface is primordial in the analysis of the solidification process, being necessary its determination. There are several methods to solve this problem. The method based on the theoretical-experimental fit of thermal profiles, used in this work, consists of accomplishing experimental thermal profiles in the mold and/or in the metal along the solidification process and, afterwards, to confront them with those furnished by theoretical solidification heat transfer models [6,7,8].

The method used to determine the transient metal/coolant heat transfer coefficient, h, is based on the solution of the Inverse Heat Conduction Problem (IHCP)[6]. This method makes a complete mathematical description of the physics of the process and is supported by temperature measurements at known locations inside the heat conducting body. The temperature files containing the experimentally monitored temperatures are used in a finite difference heat flow model to determine h, as described in a previous article[8]. The process at each time step included the following: a suitable initial value of h is assumed and with this value, the temperature of each reference location in casting at the end of each time interval Δt is simulated by using an implicit finite difference technique. The correction in h at each interaction step is made by a value Δh, and new temperatures are estimated $[T_{est}(h+\Delta h)]$ or $[T_{est}(h-\Delta h)]$. With these values, sensitivity coefficients (ϕ) are calculated for each interaction, given by:

$$f = \frac{T_{est}(h + \Delta h) - T_{est}(h)}{\Delta h_1} \quad (12)$$

The procedure determines the value of h, which minimizes an objective function defined by:

$$F(h) = \sum_{i=1}^{n} (T_{est} - T_{\exp})^2 \quad (13)$$

where T_{est} and T_{exp} are the estimated and the experimentally measured temperatures at various thermocouples locations and times, and n is the iteration stage. The method has been used in recent publications for determining h for a number of solidification situations [6].

EXPERIMENTAL PROCEDURE

The experimental apparatus consists of a horizontal cylindrical chill made of stainless steel

as schematically shown in Figure 4. After the metal melts, the mold is taken off of the heating system and is cooled by water.

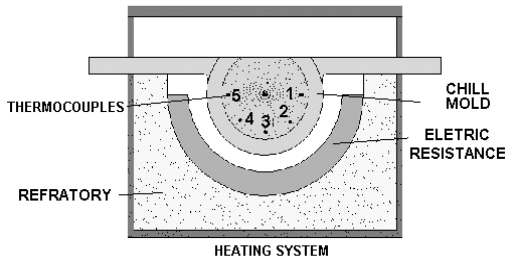

Figure 4. Schematic representation of the experimental setup and thermocouple positions.

For monitoring the temperatures, a recording microprocessor system with 16 channels was used and J type thermocouples (iron-constantan) were placed longitudinally along the section at points located 5mm from the metal/mold interface and subsequently 45 degrees equidistant of each other, as shown in figure 4. The cooling system was designed in such way that the water flow guarantees an extraction of heat essentially radial during solidification. The water flow was kept constant about 20 l/min, controlled by a rotameter. Figure 5 shows a perspective view of the cooled chill mold used in the experiments, while figure 6 shows its cross section with the respective dimensions.

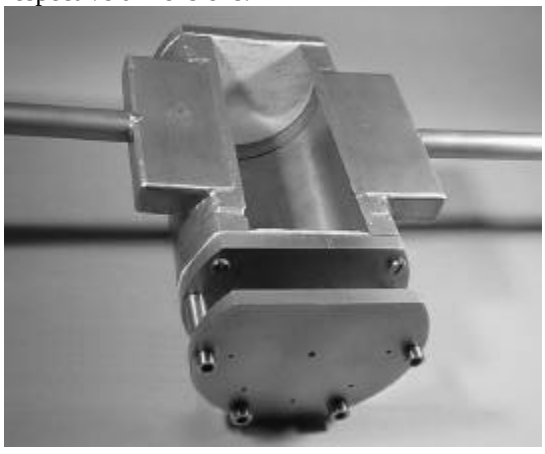

Figure 5. Stainless Steel Chill Mold.

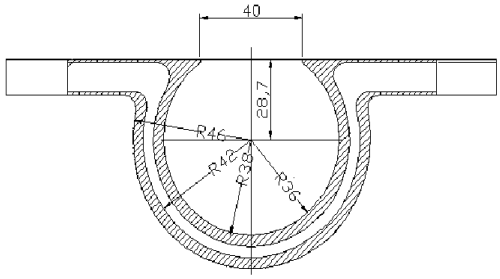

Figure 6. Cross section and dimensions of the Chill Mold [mm].

For the experimental analysis, Sn5wtPb and Sn15wtPb alloys were used, with melt superheats of 3% and 20% above the liquidus temperature. A solution containing 55g of $FeCl_3$ and 4 ml HCl for each 150 ml of water was used to reveal the ingot macrostructure. The thermo-physical properties of the alloys used in the simulations performed with the developed solidification model are shown in Table 1.

Table 1. Thermophysical properties: [9-13].

	Sn5wtPb	**Sn15wtPb**	**Eutetic**
k_S	65.4	62.2	54.4
k_L	32.8	32.5	31.7
ρ_S	7184	7906	8875
ρ_L	7184	7551.7	8434
c_S	216.4	207.3	185.4
c_L	253	240.9	211.9
L	58985	55534	47253
T_L	225	210	-
T_E	183	183	183
T_F	232	232	-
K_o	0.0656	0.0656	0.0656

RESULTS AND DISCUSSION

The temperature measurements have shown that the experimental apparatus permitted an essentially constant melt temperature to be attained before the beginning of cooling, avoiding hence, different melt superheats inside the casting. The columnar structure in the radial direction reveals a typical radial heat flow, as shown in figure 7. An asymmetry can be seen in the macrostructure, as well as the end of the solidification that occurs above the geometric center of the casting, indicating variation of heat flow at the metal/mold interface along the cylinder cross section. The structure indicates that the heat transfer was more effective at the bottom,

decreasing along the cylinder surface toward the top (figure 7).

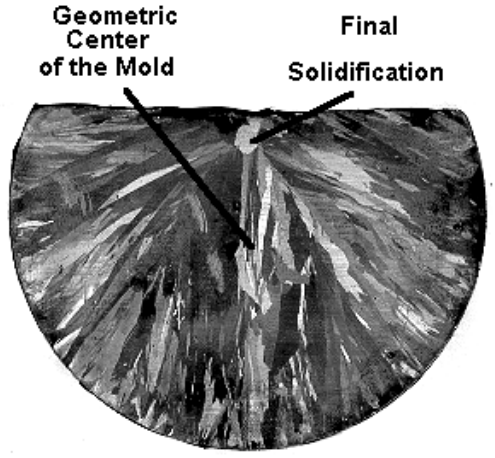

Figure 7. Typical macrostructure of the cylindrical casting cross section : Sn5wt%Pb, Tp= 252 °C.

The effect of metal contraction in the formation of the air gap is better visualized by means of the experimental temperatures profiles monitored in different points inside the casting located at 5 mm from the metal/mold interface. The different heat transfer coefficients were determined through an automatic search of the best fit between experimental and numerically predicted thermal profiles, as detailed in a previous article [6]. Figures 8 through 11 show the comparison between experimental thermal responses and those simulated for the Sn5wtPb and Sn15wtPb alloy castings, with 3% and 20% of melt superheat. In order to parametrize h with time, the software Microcal Origin was used which is based on the Classical Freundlinch Model of least square minimization.

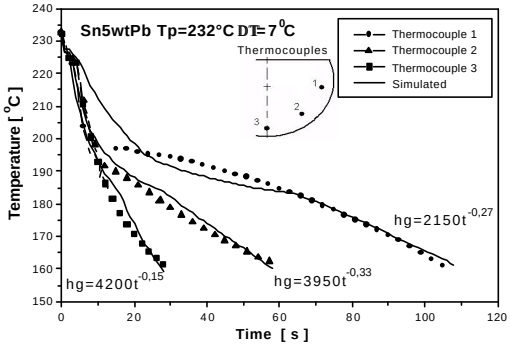

Figure 8. Experimental and simulated temperatures. Sn5wtPb.Tp= 232 °C.

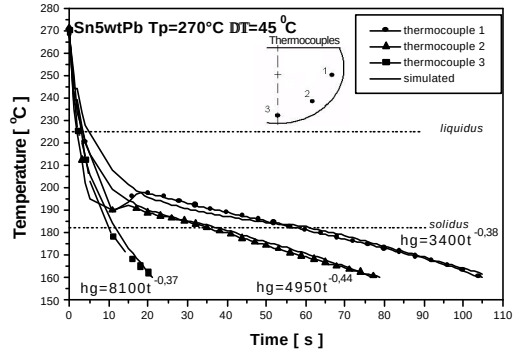

Figure 9. Experimental and simulated temperatures. Sn5wtPb.Tp= 270 °C.

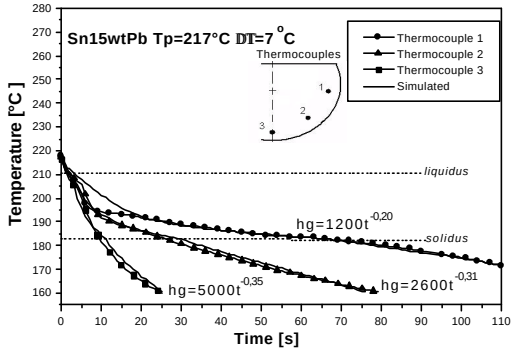

Figure 10. Experimental and simulated temperatures. Sn15wtPb.Tp= 217 °C.

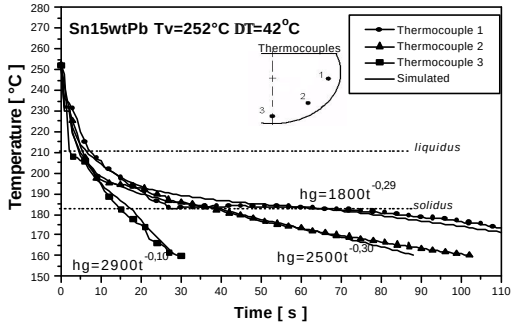

Figure 11. Experimental and simulated temperatures. Sn15wtPb.Tp= 252 °C.

The results of thermal analysis show a decrease of the thermal contact between the metal and the mold, with the angular variation toward the casting top. The metal contraction at the ingot bottom is less pronounced than at the other regions due to the the gravitational effect. Tables 2 and 3 show the resulting equations describing the metal/mold transient heat transfer coefficients

(h), at characteristic positions along the cylinder cross section. They express h as a power function of time, given by:

$$h = a.t^{-n}$$

where:

- t is the time;
- n and a are constants which depend on alloy composition and solidification conditions.

Table 2. Transient heat transfer coefficients for Sn5wtPb cylindrical castings.

Position	**Sn5wtPb**	
	Tp=232°C	**Tp=270°C**
1 (lateral)	$h=2150.t^{-0,27}$	$h=3400.t^{-0,38}$
2 (45°)	$h=3950.t^{-0,33}$	$h=4950.t^{-0,44}$
3 (bottom)	$h=4200.t^{-0,15}$	$h=8100.t^{-0,37}$

Table 3. Transient heat transfer coefficients for Sn15wtPb cylindrical castings.

Position	**Sn15wtPb**	
	Tp=217°C	**Tp=252°C**
1 (lateral)	$h=1200.t^{-0,20}$	$h=1800.t^{-0,35}$
2 (45°)	$h=2600.t^{-0,31}$	$h=2500.t^{-0,30}$
3 (bottom)	$h=5000.t^{-0,35}$	$h=2900.t^{-0,10}$

The variation of the heat transfer coefficient as a function of time, are shown in figures 12, 13, 14 and 15. It can be seen that a significant difference in metal/mold heat transfer efficiency exists along the cross section of horizontal cylindrical castings. The difference is greater between positions 1 and 3, due to the progressive decrease of the gravitational influence.

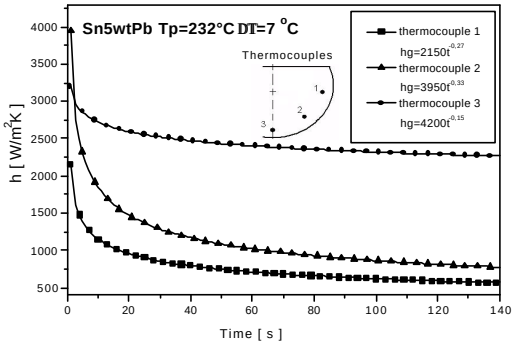

Figure 12. Variation of the heat transfer coefficient with time. Sn5wtPb. Tp=232 °C.

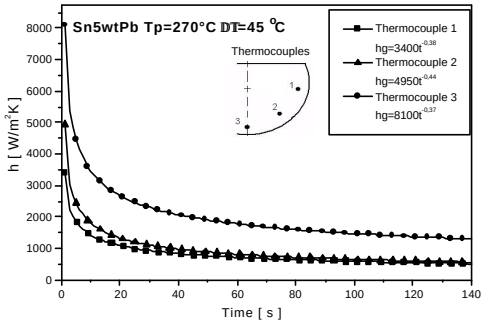

Figure 13. Variation of the heat transfer coefficient with time. Sn5wtPb. Tp=270 °C.

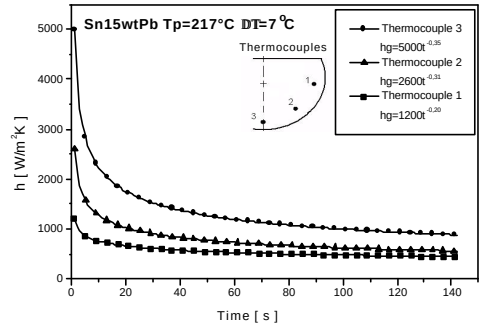

Figure 14. Variation of the heat transfer coefficient with time. Sn15wtPb. Tp=217 °C.

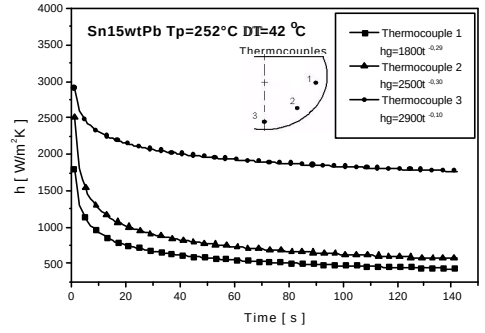

Figure 15. Variation of the heat transfer coefficient with time. Sn15wtPb. Tp=252 °C.

The influence of alloy composition on metal/mold heat transfer coefficient is shown in Figure 16. Most of the time, Sn5wtPb alloy presents h values higher than the Sn15wtPb alloy, except for the initial h values. At the initial stage of solidification (a period of about 3 seconds), the wetting of the mold by the Sn15wtPb melt seems to be more effective, translating into higher initial heat transfer coefficients.

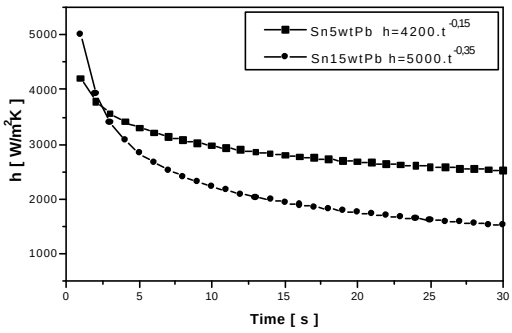

Figure 16. Heat transfer coefficient as a function of time for different alloy compositions: bottom part of the mold (position 3). Melt superheat: 3% above liquidus temperature.

CONCLUSIONS

Experiments were conducted to analyze the behavior of metal-mold heat transfer coefficients (h) during solidification of Sn-Pb alloys in a cylindrical stainless steel chill. The following conclusions can be drawn:

- The transient interfacial heat transfer coefficient (h) has been characterized by using an approach based on measured temperatures along casting and chill, and numerical simulations provided by a heat flow model based on IHCP procedure.
- The metal-mold heat transfer coefficients have also been expressed as a power function of time, given by the general form:

$$h = a.t^{-n}$$

-The determination of heat transfer coefficients with angular position in cylindrical systems provides more precise solidification information useful for conventional foundry and continuous casting processes.

-The heat flow variation at the metal/mold interface, is dependent on the thermal contraction, the gravitational effect and the alloy composition, and influences the morphology of the structure. The thermal contact is more effective at the bottom, decreasing along the cylinder surface toward the top of the mold.

REFERENCES

1. G. Fortin, P. R. Louchez and F. H. Samuel, Evolution of the heat transfer during the radial solidification of puree aluminium. *La Revue of Métallurgie-CIT/ScienceetGénie gives Matériaux***,** 772 (1994)

2. M. Trovant and S. Argylopoulos, Finding boundary conditions: the coupling strategy goes the modeling of metal casting you process: part I. experimental study and correlation development. *Metallurgical and Materials Transactions B*, **31**, 75 (2000)

3. T. G. Kim and Z. H. Lee, Team-varying heat transfer coefficients between tube-shaped casting and metal mold. *International Journal Heat Transfer Mass, v.40*, **15**, 3513 (1997)

4. E. N. Souza, *Desenvolvimento de um Equipamento de Lingotamento Contínuo Horizontal para Metais Não-Ferrosos:* MSc thesis, Porto Alegre, p.140.

5. F. P. Incropera and D.P. Dewitt, *Fundamentals of Heat and Mass Transfer*.3 ed. John Wiley & Sons, Singapore, 1990, p.58.

6. C. A. Santos, J. M. V. Quaresma and A. Garcia, Determination of transient interfacial heat transfer coefficients in chill mold castings, *Journal of Alloys and Compounds*, **319**, 174 (2001)

7. A. Garcia, *Solidificação Fundamentos e Aplicações*, Editora da Unicamp, Campinas, 2001, p. 399.

8. M. Krishnan, D. G. R. Sharma, Int. Comm. Heat Mass Transfer, **23**, 203 (1996)

9. L.F. Mondolfo, Marerials Science and Technology, **5**, 118 (1976)

10. R.D. Pehlke et al., Summary of Thermophysical Properties for Casting Alloys and Mold Materials, University of Michigan, 1982.

11. Y.S. Toloukian et al., in: Thermophysical Properties of Matter, v.1, IFI/Plenum, New York, 1970.

12. A. Benjan, Heat Transfer, Wiley, New York, 1993.

13. D. Bouchard, J.S. Kirkaldy, Metallurgical Transactions, 28B, 651 (1997)

14. R. Hadden and B. Indyk, Heat transfer characteristic in closed head horizontal continuous casting. *The Metals Society*, London, 250 (1979)

15. H. Huang, J. L. Hill, V. K. Suri, V. Berry and R. D. Pehlke, Modeling the variation and distribution of the air gap heat transfer coefficient in shaped castings. *The Minerals, Metals and Materials Society*, 65 (1991)

16. W. D. Griffiths, A model of the interfacial heat-transfer coefficient during unidirectional solidification of an aluminum alloy. *Metallurgical and Materials Transactions B*, **31B**, 285 (2000)

17. D. S. Riley, F. T. Smith and G. Poots, The inward solidification of spheres and circular

cylinders, *International Journal Heat Mass Transfer*, **v.17**, 1507 (1974)

18. P. M. Becket and N. Hobson, The effect of shrinkage on the rate of solidification of a cylindrical ingot, *International Journal Heat Mass Transfer*, **v.23**, 433 (1980)

19. J. F. Evans, D. H. Kirkood and J. Beech, The determination of metal/mold interfacial heat transfer coefficients and the prediction of gross shrinkage cavities in chill mold castings, *The Minerals, Metals & Materials Society*, 531 (1991)

20. R. G. Santos and A. Garcia, Thermal behaviour during the inward solidification of cylinders and spheres and correlation with structural effects, *Int. J. Cat Metals Res*., **11**, 187 (1998)

21. E. Çadirli and M. Gündüz, The directional solidification of Pb-Sn alloys, *Journal of Materials Science*, **35**, 3837 (2000)

22. O. M. Haddad, M. Al-Nimr and M. Siliet, The effect of gas-gap formation due to shrinkage on the rate of heat transfer during solidification, *Numerical Heat Transfer, Part A*, **40**, 887 (2001)

23. F. Lau, W. B. lee, S. M. Xiong and B. C. Liu, A study of the interfacial heat transfer between an iron casting and a metallic mold, Journal of Materials Processing Technology, 79, 25 (1998)